References and Notes

1. M. Essex, G. Klein, S. P. Snyder, J. B. Harrold, *Nature (London)* **233**, 195 (1971).
2. ———, *Int. J. Cancer* **8**, 384 (1971).
3. M. Essex, *Contemp. Top. Immunobiol.* **6**, 71 (1976).
4. ———, J. R. Stephenson, W. D. Hardy, Jr., S. M. Cotter, S. A. Aaronson, *Proceedings of the Cold Spring Harbor Conference on Cell Proliferation*, in press.
5. J. R. Stephenson, M. Essex, S. Hino, W. D. Hardy, Jr., S. A. Aaronson, *Proc. Natl. Acad. Sci. U.S.A.* **74**, 1219 (1977).
6. M. Essex, F. de Noronha, S. Oroszlan, W. D. Hardy, Jr., in *Proceedings of the Third International Symposium on Detection and Prevention of Cancer*, H. E. Nieburgs, Ed. (Dekker, New York, in press).
7. I. C. Henderson, M. M. Lieber, G. Todaro, *Virology* **60**, 282 (1974).
8. G. Todaro, J. E. DeLarco, S. Cohen, *Nature (London)* **264**, 26 (1976).
9. M. B. Gardner, P. Arnstein, R. W. Rongey, J. D. Estes, P. S. Sarma, C. F. Rickard, R. J. Huebner, *ibid.* **226**, 807 (1970).
10. C. J. Sherr, R. E. Benveniste, M. M. Leiber, G. Todaro, *J. Virol.* **19**, 346 (1976).
11. M. Essex and S. P. Snyder, *J. Natl. Cancer Inst.* **51**, 1007 (1973).
12. W. D. Hardy, Jr., L. J. Old, P. W. Hess, M. Essex, S. M. Cotter, *Nature (London)* **244**, 266 (1973).
13. P. J. Fischinger, C. S. Blevins, S. Nomura, *J. Virol.* **14**, 177 (1974).
14. M. Essex, A. Sliski, S. M. Cotter, R. M. Jakowski, W. D. Hardy, Jr., *Science* **190**, 790 (1975).
15. M. Essex, A. Sliski, W. D. Hardy, Jr., S. M. Cotter, *Cancer Res.* **36**, 640 (1976).
16. M. Essex, S. M. Cotter, J. L. Carpenter, W. D. Hardy, Jr., P. Hess, W. Jarrett, D. S. Yohn, *J. Natl. Cancer Inst.* **54**, 631 (1975).
17. C. K. Grant, D. J. DeBoer, M. Essex, M. B. Worley, J. Higgins, *J. Immunol.*, in press.
18. W. Jarrett, O. Jarrett, L. Mackey, H. Laird, C. Hood, D. Hay, *Int. J. Cancer* **16**, 34 (1975).
19. R. G. Olsen, E. A. Hoover, L. E. Mathes, L. Heding, J. P. Schaller, *Cancer Res.* **36**, 3642 (1976).

20. We thank K. DeSanti and J. Michaud for technical assistance, Dr. J. Whitescarver and C. Ramaika for photography, and Drs. F. de Noronha, W. D. Hardy, Jr., J. R. Stephenson, and S. A. Aaronson for serum reagents. Supported by grants CA-13885, CA-18216, and CA-09031, and contract CB-64001 from the National Cancer Institute, and grant PDT-36A from the American Cancer Society. M.E. is a scholar of the Leukemia Society of America.

3 January 1977; revised 3 February 1977

Potential Operating Region for Ultrasoft X-ray Microscopy of Biological Materials

Abstract. *Calculations are presented which indicate an extensive suboptical region in the microscopy of biological materials in their natural state which is accessible to ultrasoft x-ray transmission microscopy. Throughout most of the region, radiation dosage levels to the specimen are lower than in electron microscopy.*

It has been shown in recent work (*1*) that contact microradiography with the use of ultrasoft x-rays and high-resolution polymer resist detectors is capable of resolutions of the order of 100 Å with unstained biological materials. Similarly, the feasibility of ultrasoft x-ray microscopy with the use of Fresnel zone-plates and of scanning microscopy with synchrotron x-rays has been shown (*2*, *3*), although at lower resolutions than the above. These accomplishments suggest the desirability of ascertaining just what the potential operating region for ultrasoft x-ray transmission microscopy may be.

As a contribution to the study of this question we have calculated the radiation dose D which an unstained biological specimen must undergo in ultrasoft x-ray microscopy. [It is known (*4*) that radiation dose and the damage resulting therefrom is the limiting factor in the resolution obtainable by electron microscopy of unstained biological systems.] The calculations cover bright-field and dark-field transmission x-ray microscopy, a wavelength range for the photons from 1.3 to 90 Å, and model systems representative of a number of different simplified two- and three-phase biological specimens. The dose D is calculated as a function of the specimen thickness t and the resolution d at which the microscopy is being carried out. It is assumed in the calculations that the instrumentation is ideal in the sense that it does not increase dosages over those calculated (for example, through losses in the detectors) or decrease resolution (for example, through diffraction effects or through aberrations in the optical elements).

For convenience in comparing with electron microscopy, D is similarly calculated for an extensive set of CTEM and STEM modes (*5*), and for electron energies in the range 10^4 to 10^7 ev. Analogous assumptions are made about the freedom of the instrumentation from signal and resolution loss.

Under the assumptions given, the minimum incident flux $n_{\min}$ of particles on the specimen necessary to distinguish reliably between two differing resolution elements of the specimen is given by

$$n_{\min} = 25(p_1 + p_2)/d^2(p_1 - p_2)^2 \quad (1)$$

where d is the edge-length of the resolution element, and p_1, p_2 are the probabilities of an incident particle giving rise to an event of the type being used to form the signal in the microscopy in question in the two resolution elements. Equation 1 is a modified form of the criterion originally introduced by Rose (*6*). For ultrasoft x-rays the event may be the transmission of the photon through the specimen (bright-field microscopy, mode X1 in our nomenclature), or the absorption of the photon in the specimen (dark-field microscopy, mode X2).

If one assumes that the resolution elements consist of a background material B of thickness t_B and a feature material, which is F1 or F2 in the two different types of resolution element, of thickness t_F, then

$$p_1^{X1} = \exp(-\mu_B t_B - \mu_{F1} t_F), \qquad p_2^{X1} = \exp(-\mu_B t_B - \mu_{F2} t_F) \quad (2a)$$

and

$$p_1^{X2} = 1 - \exp(-\mu_B t_B - \mu_{F1} t_F), \qquad p_2^{X2} = 1 - \exp(-\mu_B t_B - \mu_{F2} t_F) \quad (2b)$$

for X1 and X2 microscopy, respectively. Here μ_B, μ_{F1}, and μ_{F2} are the linear absorption coefficients for the x-rays in question in the materials in question, and may be calculated from tabulated data (*7*). Together, Eqs. 1 and 2 allow the minimum flux of photons to be calculated in terms of the thicknesses of background and features in the specimen, the wavelength of the x-rays and materials of the background and features, the mode of the microscopy, and the desired resolution d.

The mean radiation dosage (energy deposited per unit mass) in the initial layers of a specimen composed of equal numbers of elements containing F1 and F2, corresponding to the minimum incident flux $n_{\min}$, is

$$D = n_{\min}\bar{E}\,[2\mu_B t_B + (\mu_{F1} + \mu_{F2})\,t_F] \,/\, [2\rho_B t_B + (\rho_{F1} + \rho_{F2})t_F] \quad (3)$$

where $\bar{E}$ is the energy deposition per absorption $h\nu$ and ρ_B, ρ_{F1}, ρ_{F2} are the densities of the materials B, F1, F2, respectively. With the aid of Eq. 3, the least dosage to the specimen consistent with reliable imaging can be calculated in terms of the quantities noted above (thicknesses and materials of specimen, wavelength, mode, and resolution).

In electron microscopy, Eq. 2 is replaced by formulas corresponding to the eight CTEM and STEM modes considered (*5*). The formulas are similar to Eq. 2 in form, but involve the linear coefficients for elastic scattering μ_B^e, μ_{F1}^e, μ_{F2}^e and inelastic scattering μ_B^i, μ_{F1}^i μ_{F2}^i. The linear coefficients are calculable from the atomic cross sections for elastic and inelastic scattering (*8*). Finally, Eq. 3 is modified in the electron case by reducing $\bar{E}$ to approximately 48 ev [this choice yields values for the dose which are in close agreement with relativistic stopping power equation values (*4*, *9*)], and replacing μ's by μ^i's.

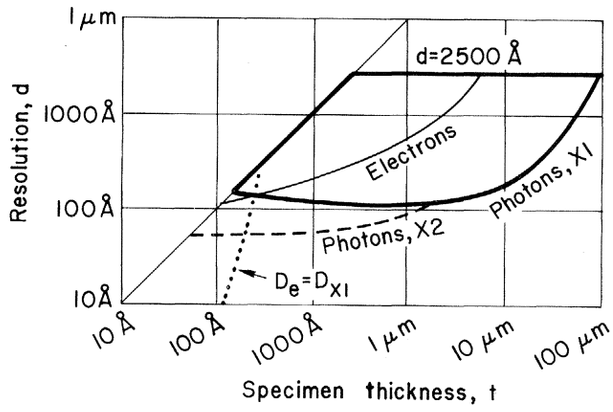

Fig. 1. Contours in the (t, d)-plane (where t is the specimen thickness and d is the resolution) of the radiation dose that must be undergone by a specimen consisting of protein features in a water background. Contours are at 10^9 rads. The area bounded by heavy solid lines is the potential suboptical operating region (for the protein-water specimens) for bright-field transmission microscopy with ultrasoft x-ray photons. Other curves are described in the text.

Figure 1 summarizes some of the major results for a typical specimen. consisting of equidimensional ($t_F = d$) protein features in a water background (B = F1 = water, F2 = protein). The coordinates of the figure are specimen thickness t ($t = t_B + t_F$) and resolution d. As has been noted above, the minimum dose D is a function of (t, d). The principal curves in the figure are contours of D at 10^9-rad dosage for different types of microscopy. [In each case, the particle energy or wavelength (in the electron case, mode of microscopy as well) has been chosen at each point (t, d) to give the lowest possible value for D.] Although not shown, D increases in each case as one moves downward and to the right in the figure. Since 10^9 rads represents roughly the maximum dosage consistent with structural survival of an unfixed biological specimen (*4*), the potential operating region in each case is the region above and to the left of the contour corresponding to that case.

The potential suboptical operating region for photons in mode X1 (bright-field transmission microscopy) for the protein-water system is the large area in Fig. 1 bounded by heavy solid lines. It extends to resolutions of the order of 100 Å, and covers a very wide range of specimen thicknesses.

As previously noted, the X1 photon curve is optimized at every point over photon wavelength (1.3 to 90 Å). The optimum photon wavelength starts at 43.6 Å (carbon absorption edge) at the left-hand edge of the figure and decreases as one moves to the right, reaching 23.3 Å (oxygen absorption edge) in the right-hand portion of the area shown. Thus the optimum photons for this system fall, as might be expected, in the wavelength region in which the protein feature is relatively opaque in comparison with the water background.

The operating region for electrons is smaller than that for X1 photons, but extends to slightly better resolutions for thin specimens ($t < 350$ Å). The electron curve is optimized at each point over the four CTEM and four STEM modes and over electron energy (10^4 to 10^7 ev).

The trace of the point of intersection of the electron and X1 photon curves is shown in Fig. 1. To the left of this trace electrons image the protein-water system with smaller dosage than do mode X1 photons, while to the right the opposite is true. The dosage advantage of the X1 photon increases to approximately $10^4 : 1$ along the line $t = 5$ μm.

The curve marking the 10^9-rad contour for photons in mode X2 extends the operating area for photons considerably to the lower left. Under these circumstances photons image with a dosage advantage of at least 10 : 1 everywhere in the plane. It must be pointed out, however, that the feasibility of X2 microscopy is uncertain, except perhaps in the case of very thin specimens, because of the short range of those products (photoelectrons, Auger electrons) of the absorption events which are produced in high yield. It should also be noted that diffraction effects may make the contour unrealistic as drawn (the optimizing wavelength for the photons, as in the X1 case, is 43.6 Å in the left-hand portion of the contour).

Physically, the results of Fig. 1 reflect the balance between the lower average energy transfer per event in the case of the electron and the lower number of events required to effect feature recognition in the case of the photon. The latter in turn arises from the greater selectivity of the photon in its interaction with the electrons of the specimen according to their binding energies.

It should be noted that we have implicitly assumed that radiation dose in the specimen is a reliable index of specimen damage. It is likely, in fact, that a given dose is somewhat more damaging if delivered by ultrasoft x-rays than by electrons. As a result of such considerations, slight repositionings of the curves presented may be required to allow for their direct interpretation in terms of damage, but we believe no significant effect on the conclusions that may be drawn will result.

Details of the theory and calculations, as well as results on other two- and three-phase systems in which F1 and F2 are drawn from the list (water, protein, carbohydrate, lipid, nucleic acid), will be published elsewhere (*10*). The case in which the incident flux of particles is noise-free, which produces a slight improvement in the electron case, will also be treated in that paper.

D. SAYRE

IBM Research Center, Yorktown Heights, New York 10598

J. KIRZ

Department of Physics, State University of New York, Stony Brook 11794

R. FEDER

IBM Research Center

D. M. KIM

Department of Electrical Engineering, Rice University, Houston, Texas 77001

E. SPILLER

IBM Research Center

References and Notes

1. R. Feder, E. Spiller, J. Topalian, A. N. Broers, W. Gudat, B. J. Panessa, J. Sedat, *Science*, in press; see → E. Spiller, R. Feder, J. Topalian, D. Eastman, W. Gudat, D. Sayre, *ibid.* **191**, 1172 (1976).
2. B. Niemann, D. Rudolph, G. Schmahl, *Appl. Optics* **15**, 1883 (1976).
3. P. Horowitz and J. A. Howell, *Science* **178**, 608 (1972).
4. See, for example, R. M. Glaeser, in *Physical Aspects of Electron Microscopy and Microbeam Analysis*, B. M. Siegel and D. R. Beaman, Eds. (Wiley, New York, 1975), p. 205.
5. The modes are C1 to C4 and S1 to S4 as listed by A. V. Crewe and T. Groves [*J. Appl. Phys.* **45**, 3662 (1974)]. The C and S modes correspond to conventional and scanning transmission electron microscopy, respectively. C1 and S1 are bright field (U + I), C2 and S2 are bright field with energy filtering (U), C3 and S4 are dark field (E + EI), S3 is dark field with inelastic electrons only (I), C4 is dark field with energy filtering (E). (The notations in parentheses give the composition of the image-forming signal, with U = unscattered, E = elastically scattered, I = inelastically scattered, and EI = elastically and inelastically scattered.) In our treatment we have idealized the instrumentation slightly over that of Crewe and Groves by assuming perfect separation of the U, E, I, and EI signals.
6. A. Rose, *J. Soc. Motion Pict. Eng.* **47**, 273 (1946).
7. B. L. Henke and E. S. Ebisu, *Adv. X-Ray Anal.* **17**, 150 (1974).
8. Formulas for μ^e and μ^I, respectively, are given by J. P. Langmore, J. Wall, and M. S. Isaacson [*Optik* **38**, 335 (1973)]; and M. S. Isaacson [in *Physical Aspects of Electron Microscopy and Microbeam Analysis*, B. M. Siegel and D. R. Beaman, Eds. (Wiley, New York, 1975), p. 247].
9. R. M. Glaeser, *J. Ultrastruct. Res.* **36**, 466 (1971).
10. D. Sayre, J. Kirz, R. Feder, D. M. Kim, E. Spiller, *Ultramicroscopy*, in press.
11. We gratefully acknowledge an NSF faculty research participation program grant enabling one of us (D.M.K.) to spend a period of time at the IBM Research Center.

28 December 1976; revised 13 April 1977